Eur J Vasc Endovasc Surg (2017) 54, 254–263

In Silico Shear and Intramural Stresses are Linked to Aortic Valve Morphology in Dilated Ascending Aorta

S. Pasta [a,b,*], G. Gentile [c], G.M. Raffa [b], D. Bellavia [b], G. Chiarello [d], R. Liotta [d], A. Luca [c], C. Scardulla [b], M. Pilato [b]

[a] Fondazione Ri.MED, Palermo, Italy
[b] Department for the Treatment and Study of Cardiothoracic Diseases and Cardiothoracic Transplantation, IRCCS-ISMETT, Palermo, Italy
[c] Department of Diagnostic and Therapeutic Services, IRCCS-ISMETT, Palermo, Italy
[d] Department of Pathology, IRCCS-ISMETT, Palermo, Italy

WHAT THIS PAPER ADDS
The use of computational modeling for risk stratification of aortic dilatation is a very promising approach.

Objective/Background: The development of ascending aortic dilatation in patients with bicuspid aortic valve (BAV) is highly variable, and this makes surgical decision strategies particularly challenging. The purpose of this study was to identify new predictors, other than the well established aortic size, that may help to stratify the risk of aortic dilatation in BAV patients.
Methods: Using fluid–structure interaction analysis, both haemodynamic and structural parameters exerted on the ascending aortic wall of patients with either BAV ($n = 21$) or tricuspid aortic valve (TAV; $n = 13$) with comparable age and aortic diameter (42.7 ± 5.3 mm for BAV and 45.4 ± 10.0 mm for TAV) were compared. BAV phenotypes were stratified according to the leaflet fusion pattern and aortic shape.
Results: Systolic wall shear stress (WSS) of BAV patients was higher than TAV patients at the sinotubular junction (6.8 ± 3.3 N/m^2 for BAV and 3.9 ± 1.3 N/m^2 for TAV; $p = .006$) and mid-ascending aorta (9.8 ± 3.3 N/m^2 for BAV and 7.1 ± 2.3 N/m^2 for TAV; $p = .040$). A statistically significant difference in BAV versus TAV was also observed for the intramural stress along the ascending aorta (e.g., $2.54 \times 10^5 \pm 0.32 \times 10^5$ N/m^2 for BAV and $2.04 \times 10^5 \pm 0.34 \times 10^5$ N/m^2 for TAV; $p < .001$) and pressure index (0.329 ± 0.107 for BAV and 0.223 ± 0.139 for TAV; $p = .030$). Differences in the BAV phenotypes (i.e., BAV type 1 vs. BAV type 2) and aortopathy (i.e., isolated tubular vs. aortic root dilatations) were associated with asymmetric WSS distributions in the right anterior aortic wall and right posterior aortic wall, respectively.
Conclusion: These findings suggest that valve mediated haemodynamic and structural parameters may be used to identify which regions of aortic wall are at greater stress and enable the development of a personalised approach for the diagnosis and management of aortic dilatation beyond traditional guidelines.

Article history: Received 1 December 2016, Accepted 25 May 2017, Available online 24 June 2017
Keywords: Aneurysm of ascending aorta, Bicuspid aortic valve, Computational modeling, Wall shear stress

INTRODUCTION

Bicuspid aortic valve (BAV) is the most common congenital heart defect, leading to a significant healthcare burden.[1] The reported prevalence of dilatation of the ascending aorta among patients with BAV (namely "bicuspid aortopathy") is highly variable with a reported prevalence of 20–84%.[2] This variation is probably a reflection of the diverse molecular pathways, valve phenotypes, flow dynamics, and patterns of aortic dimension characterising the BAV disease.

The rate of abnormal dilatation observed in the ascending aorta is higher in patients with bicuspid vs. tricuspid aortic valve (TAV).[3] With an understanding that BAV leads to greater risk of aortic dissection or rupture, there are currently no reliable predictors to better inform clinicians whether an aggressive approach is appropriate.[4] The most challenging questions for surgeons often arise with decisions whether to prophylactically resect a moderately dilated aorta in those individuals with a normally functioning BAV. In this case, the risk/benefit ratio of an aggressive strategy, aimed at carrying out surgery on a better preserved cusp structure, has not yet been clarified.[5] Recently, classification schemes that are based on morphological valve fusion patterns have been proposed as potential criteria for risk stratification of bicuspid aortopathy.[6,7] Similarly, four dimensional (4D) flow magnetic resonance imaging (MRI) has provided some insight into haemodynamic mechanisms potentially involved in the development of BAV associated aortopathy.[8] However,

* Corresponding author. Fondazione Ri.MED, Via Bandiera n.11, 90133 Palermo, Italy.
E-mail address: spasta@fondazionerimed.com (S. Pasta).

http://dx.doi.org/10.1016/j.ejvs.2017.05.016

none of the proposed classification schemes is currently adopted in clinical practice; large prospective studies are warranted to assess the potential of 4D flow MRI.

It was hypothesised that haemodynamics and aortic wall structural variables are useful in the risk stratification of aortic dilatation, specifically occurring in patients with BAV. Therefore, the present study aimed to compare computationally derived haemodynamics and structural variables that are exerted on the dilated ascending aorta of patients without any concomitant cardiovascular diseases other than BAV or TAV. The role of different BAV phenotypes and patterns of aortic shape was also investigated.

METHODS

Study population and computed tomography imaging

After internal review board approval and informed consent, a total of 21 BAV patients and 13 TAV patients referred for aortic size evaluation by electrocardiogram (ECG) gated computed tomography angiography (CTA) were enrolled. Patient exclusion criteria were: arterial hypertension; connective tissue disorders in the medical history or thorax deformations; medication or past surgery; greater than mild aortic stenosis or aortic regurgitation assessed by ECG. This was carried out to form a homogeneous and strict study group of individuals with as few confounding variables as possible influencing haemodynamics in the dilated ascending aorta. Elective surgical repair of aneurysmal aorta was carried out for six BAV patients and five TAV patients with aortic sizes of 48.5 $\pm$ 1.6 mm and 51 $\pm$ 3.6 mm, respectively.

Measurements of aortic dimension and geometry

For all patients, aortic diameters were measured at the sinus of Valsalva (D_{sinus}), sinotubular junction (D_{STJ}), and mid-ascending aorta (D_{asc}) by experienced radiologists using standard of care imaging. Measurements were collected on oblique-sagittal images reconstructed at the mid-diastolic phase for the aortic root and ascending thoracic aorta. To assess aortic valve morphology, ECG gated CTA scans were reconstructed to obtain images at cardiac phases corresponding to diastole and systole.[9] Each aortic valve was analysed and characterised on the basis of reconstructed images parallel to the aortic valve plane. BAV was defined as the presence of two cusps and commissures, with or without raphe in either structure. Schaefer's classification scheme of aortic shape and leaflet cusp fusion was adopted.[7] In brief, BAV type 1 was classified as fusion of the right and left coronary cusp, whereas BAV type 2 was defined as fusion of the right and non-coronary cusp. There was no observation of fusion of the left and non-coronary cusp (BAV type 3) in this group. Aortic measurements were used to group dilated aortas as: type N when $D_{sinus} > D_{STJ}$ and $D_{sinus} \geq D_{asc}$, as showed by dilatation of aortic root; type A when $D_{sinus} > D_{STJ}$ and $D_{sinus} < D_{asc}$, as shown by involvement of tubular portion of ascending aorta; type E when $D_{sinus} < D_{STJ}$, as showed by diffuse involvement of the entire ascending aorta.

Aortic tissue samples were collected as permitted by the extent of ascending aortic resection and labeled according to their anatomical location with respect to the aortic wall. Tissue samples were then embedded transversally in paraffin and cut at 5 μm thickness. Cross sections were stained by haematoxylin and eosin (H&E) and imaged by light microscopy following standard protocol by pathologists.

Computational flow analysis

Computational flow analyses were carried out using an approach previously developed by the authors' group to study the haemodynamics and wall stress of ascending thoracic aortic aneurysms by considering the aortic valve shape at systole.[10,11] In the modeling approach (see Fig. 1), realistic patient specific structural and flow conditions are integrated in a fluid—structure interaction model to diminish the impact of theoretical assumptions that are common to other computational investigations of aneurysmal aorta.[12–14] Reconstruction of aortic geometries from ECG gated CTA scans were performed using the vascular modeling toolkit ITK (https://itk.org/), as described previously.[10] The biomechanical response of the aorta was modeled using material parameters that have been determined by testing tissue samples collected from patients referred for surgical resection of dilated aorta with either BAV or TAV.[15] Therefore, the biomechanical behavior of the aorta was different for BAV patients than for TAV patients. Using a fibre reinforced constitutive model, the mechanical response of the aorta considered the collagen fibre dispersion and orientation that has been quantified using multiphoton imaging and a custom image based analysis tool to rigorously characterise the inherent fibre defect of BAV patients versus TAV patients.[16] Uniform material properties and thickness (1.8 mm for BAV and 2.0 mm for TAV) for the aortic wall were adopted. To include patient specific haemodynamics, the transaortic jet velocity evaluated by Doppler ECG was set as the inflow velocity condition at the aortic valve for each patient. The inlet flow was then split between supra-aortic vessels and descending aorta using resistances boundary conditions with values extrapolated from Kim *et al.*[17] Boundary conditions were adjusted to match the flow distribution as obtained from literature data,[18] and the measured brachial artery pulse pressure (see Fig. 1). Aortic geometries were reconstructed using semi-automatic segmentation of ECG gated CTA images with the largest aortic valve opening area, which frequently occurs 50—100 ms after the R peak.[10] Thus, reconstructions were meshed by unstructured elements at spatial resolution of 0.1 $\times$ 0.1 $\times$ 0.1 mm for both lumen and aortic wall using a resolution an order of magnitude lower than that of 4D flow MRI.

The following haemodynamic and structural variables for each analysis were evaluated: (a) the wall shear stress (WSS) in systole; (b) the pressure index (PI) as the mean of

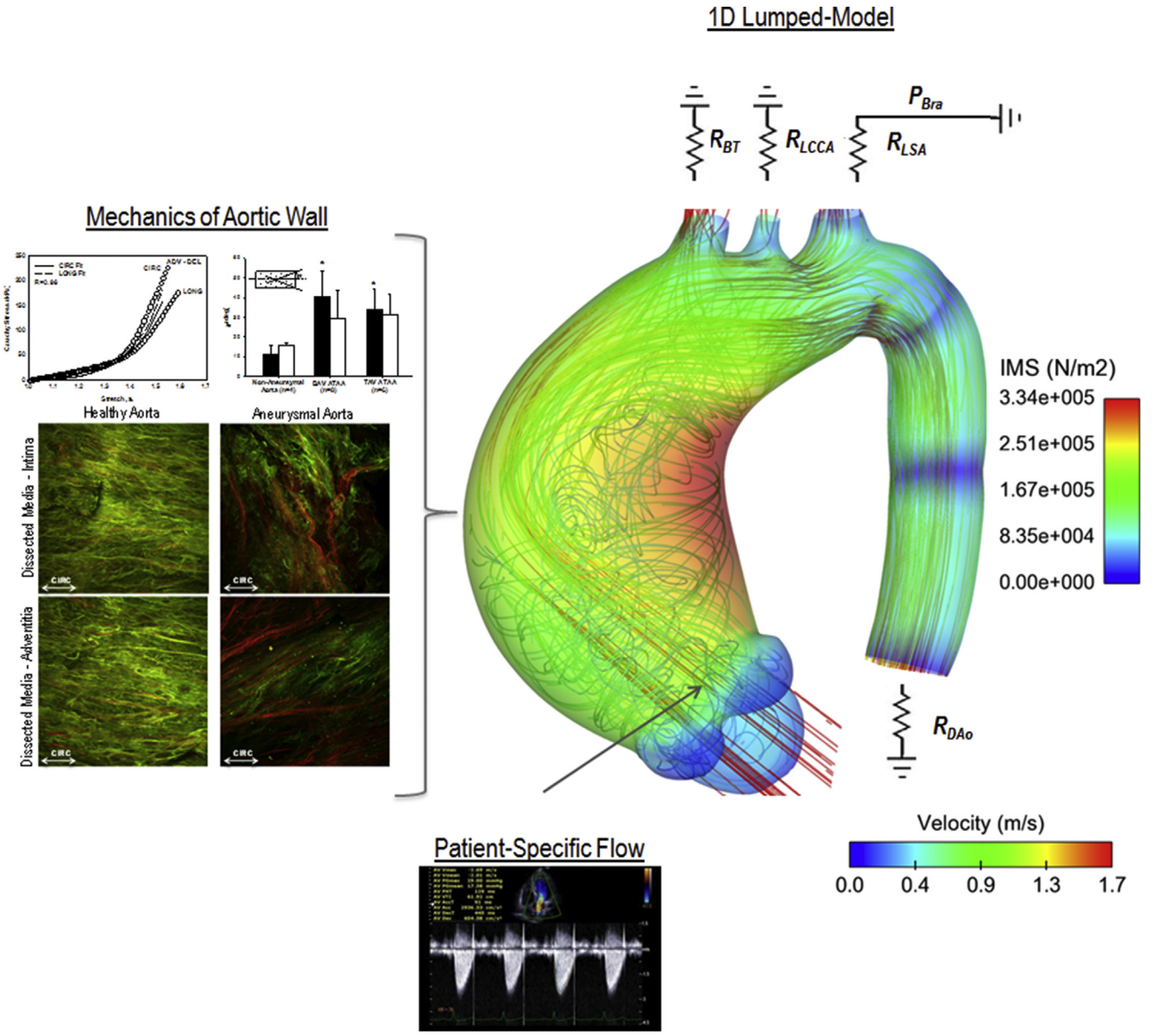

Figure 1. Illustration of fluid—structure interaction modelling of the ascending aorta. *Note*. IMS = intramural stress.

95% higher values of pressure normalised by the peak; (c) the helical flow index (HFI) as descriptor of complex, fully three dimensional flow fields according to Morbiducci *et al.* (this variable has a range of $0 \leq \text{HFI} \leq 1$ with 0 for irrotational flow);[19] (d) the intramural stress (in term of Mises stress) for the inner (IMS_{In}) and outer aortic layers (IMS_{Out}), respectively. These variables were processed using EnSight software package (v9.0; CEI, Apex, NC, USA) and then overlaid on anatomical images of thoracic aorta.

Statistical analysis

Data are shown as mean ± SD or % (*n*), depending on the variable distribution. Mann—Whitney *U*-test was used to compare both haemodynamic and structural variables between BAV and TAV patients at different analysis planes located from the sinus to the distal ascending aorta. Comparisons were also performed to assess differences in haemodynamics and structural variables between valve phenotypes (i.e., BAV type 1 vs. BAV type 2) and aortic shapes (i.e., type A vs. types N and E) for several angular segments of the aortic wall. Differences between categorical variables were assessed by Fisher's exact test. The association between aortic diameters, transaortic jet velocity, haemodynamic, and structural variables was explored using Pearson's correlation coefficients. Statistical analyses were performed using SPSS software (IBM SPSS Statistics, Armonk, NY, USA). All probability values were considered significant at the .05 threshold.

RESULTS

Patient demographics are summarised in Table 1. The distribution of age in BAV patients did not differ significantly from that of TAV patients ($p = .061$), with a male predominance of 72% ($n = 16$) in the BAV study group. There

Table 1. Descriptive statistics of patient demographics, aortic diameters, and phenotypic classification of bicuspid aortic valve (BAV) and aortic shape.

	BAV ($n = 21$)	TAV ($n = 13$)	p
Age (y)	58 ± 13	65 ± 9	.061
Male (%)	76	23	.004
AR (%)	76	44	.139
AS (%)	10	23	.348
Aortic diameters (mm)			
Sinus	37.1 ± 4.7	38.8 ± 2.6	.676
STJ	35.4 ± 6.2	38.9 ± 6.6	.132
Mid-ascending aorta	42.7 ± 5.3	45.4 ± 10.0	.451
Aortic shape (n)			
Type N	2	3	
Type A	15	7	
Type E	4	3	
BAV aortopathy (n)			
Type 1	14	—	
Type 2	7	—	
Orifice area (mm^2)	346.2 ± 88.6	447.8 ± 75.8	.003
Aortic jet flow (m/s)	2.0 ± 0.8	1.7 ± 0.6	.124

Note. Data are mean ± SD unless otherwise indicated. TAV = tricuspid aortic valve; AR = aortic regurgitation; AS = aortic stenosis; STJ = sinotubular junction.

were no significant differences in the aortic diameter for BAV vs. TAV patients at the level of sinus ($p = .676$), sinotubular junction ($p = .132$), and mid-ascending aorta ($p = .451$). The majority of BAV patients had minimal (48%) or mild (28%) regurgitation through the aortic valve and a minimal degree of aortic stenosis (10%), whereas other patients did not present any valve lesions. For TAV patients, the degree of regurgitation fraction was minimal (30%) and mild (14%), whereas the degree of aortic stenosis was minimal (16%) and mild (7%) when valve dysfunction was observed. None of patients had both mild aortic stenosis and regurgitation. Transaortic jet velocity did not statistically differ between BAV and TAV patients ($p = .124$), whereas a significant difference was noted for the orifice area between these groups ($p = .003$). Among BAV phenotypes, 14 patients had BAV type 1 and seven BAV type 2. The most prevalent aortic anatomy was type A (71%) with isolated dilatation of tubular portion of the ascending aorta, both overall and among BAV. Type N (10%) and type E (19%) were the least common. For aneurysmal aorta with TAV, seven patients had type A shape (54%), three had type N (23%), and three had type E (23%).

Flow streamlines in patients with BAV and TAV showed a remarkable association between the helical flow and the presence of BAV, with right handed helical flows common to BAV type 1 (Fig. 2). Indeed, helical flow quantification calculated with respect to the particle traces moving in the ascending aorta revealed that BAV patients had higher helical flow than TAV patients, although statistically different (HFI = 0.378 ± 0.047 for BAV and HFI = 0.361 ± 0.032 for TAV; $p = .056$). The median PI in BAV patients was found to be significantly different from that of TAV patients (0.329 ± 0.107 for BAV and 0.223 ± 0.139 for TAV; $p = .030$), suggesting that the altered BAV related flow impinges a more focused area of the aortic wall rather than an extended one as observed in TAV. The mean values of systolic WSS on each analysis plane were significantly increased at the sinotubular junction and ascending aorta of BAV study group when compared with the TAV control group (Figs. 3 and 4A). Similarly, a statistically significant difference in BAV vs. TAV patients was observed for the distribution of IMS on both the inner and outer aortic medial layers (Fig. 4B). This distribution of both WSS and IMS may participate in the dysregulation of the extracellular matrix of the aneurysmal aorta with BAV, as shown by histological observations in the aortic wall surface corresponding to high shear stress distribution. Fig. 5 shows that BAV may present aortic wall thinning characterised by the presence of atheromatous plaques in the intima and fragmentation of elastic fibres when compared with TAV.

With Pearson's correlation for the BAV study group, systolic WSS at the sinotubular junction was statistically related to the pressure parameter PI ($R = .57$; $p = .021$) and to the mid-ascending aortic diameter ($R = .76$, $p = .002$; Fig. 6A). Similarly, a positive correlation was found between IMS and mid-ascending aortic diameter in BAV patients ($R = .69$, $p = .003$ for AA1; $R = .89$, $p < .001$ for AA2; $R = .75$, $p < .001$ for AA3 [Fig. 6B]). Interestingly, BAV patients who underwent elective repair had greater IMS than non-repaired patients ($2.85 \times 10^5 \pm 0.25 \times 10^5$ N/m^2 [$n = 6$] for elective repaired aorta and $2.28 \times 10^5 \pm 0.25 \times 10^5$ N/m^2 [$n = 15$] for non-repaired aorta [$p < .001$]).

For BAV, systolic WSS distribution in the ascending aorta showed distinct differences between valve phenotypes and aortic shapes. Based on a consistent orientation of the analysis planes, systolic WSSs were calculated at eight standardised angular segments of the aortic wall. The location of significantly increased WSSs was different for BAV type 1 and BAV type 2 with the anterior—posterior morphology at high magnitude in the R and R—A segments at the sinotubular junction, as well as in the L—P, L, L—A, and A segments at analysis plane AA2 (Fig. 7A). When BAVs were grouped according to their aortic shape (Fig. 7B), significantly decreased WSSs were observed in the right quadrant for ascending tubular dilated aorta (type A) when compared with dilated aortic roots (type N) and sinus effacement aortas (type E).

DISCUSSION

The most striking finding of this study is that the entire ascending aorta of BAV patients showed greater wall shear and intramural stresses than those observed in TAV patients with comparable age and aortic size. Locally varying WSSs were associated with different patterns of both BAV fusion pattern (BAV type 1 vs. BAV type 2) and aortopathy phenotype (type A vs. type N/E). These suggest that wall stress parameters as estimated by computational modeling may be used to identify which regions of aortic wall are at greater stress and should therefore be repaired with improved strategies aimed at preserving the extent of

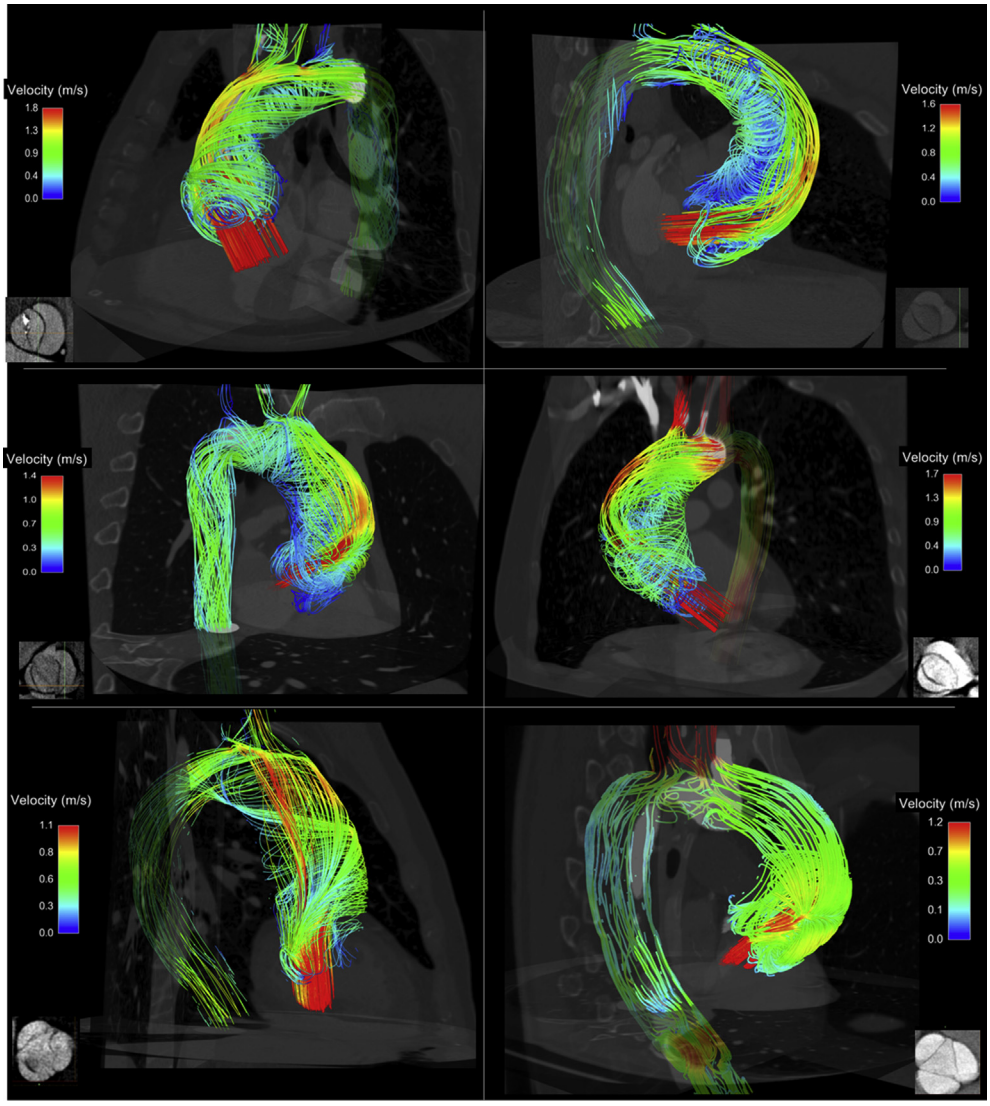

Figure 2. Flow patterns in the aorta of bicuspid aortic valve (BAV) patients (row 1 and 2) and tricuspid aortic valve (TAV) patients (row 3); patients had BAV type 1 with dilated aortic root (row 1, left), BAV type 2 with diffusive dilatation of ascending aorta (row 1, right), BAV type 2 with tubular dilatation of ascending aorta (row 2, left), BAV type 1 with tubular dilatation of ascending aorta (row 2, right).

resection. With validation, computational modeling may enable the development of an individualised approach to the diagnosis and management of aortic disease beyond traditional guidelines. None of patients investigated here had severe aortic stenosis or aortic valve regurgitation or other cardiovascular diseases, and this allowed the impact of potential cofounding variables of BAV aortopathy on the estimated haemodynamic and structural loads to be diminished.

In patients with BAV, this surgical dilemma is emphasised by clinical observations for which the progression of an aortic dilatation varies considerably among BAV phenotypes. This perspective has encouraged a more aggressive management of BAVs towards size recommendations similar to those applied in patients with Marfan syndrome or other hereditary diseases. Although the size criterion can be adjusted to achieve higher patient specificity, progress is needed toward even better metrics by the use of other parameters not based on size. For aneurysms of descending thoracic aorta, peaks of IMS correlated with expansion rates better than aortic diameter.[20] On the convex side of the ascending aorta, BAV patients exhibited increased IMS above the sinotubular junction more often than TAV patients, and increased rupture risk with elevated systolic IMS and tissue stiffness.[13] In addition, it was found that the mean values of IMS in a subgroup of BAV patients who underwent surgery was higher than those of non-repaired aneurysmal aorta patients, suggesting that IMS may be used to identify patients at high risk of complications. To differentiate BAV from TAV patients, several studies have explored the haemodynamics of the ascending thoracic aorta in BAV to potentially provide new metrics such as the restricted cusp opening angle,[21] the flow angle and flow displacement,[22] and, above all, the shear stress as derived by 4D flow MRI.[8] Helical flow patterns and regionally varying WSSs have been described in BAV patients vs. TAV patients using 4D flow MRI or computational modeling.[8,10,11,23] Aortic outflow displaced by the

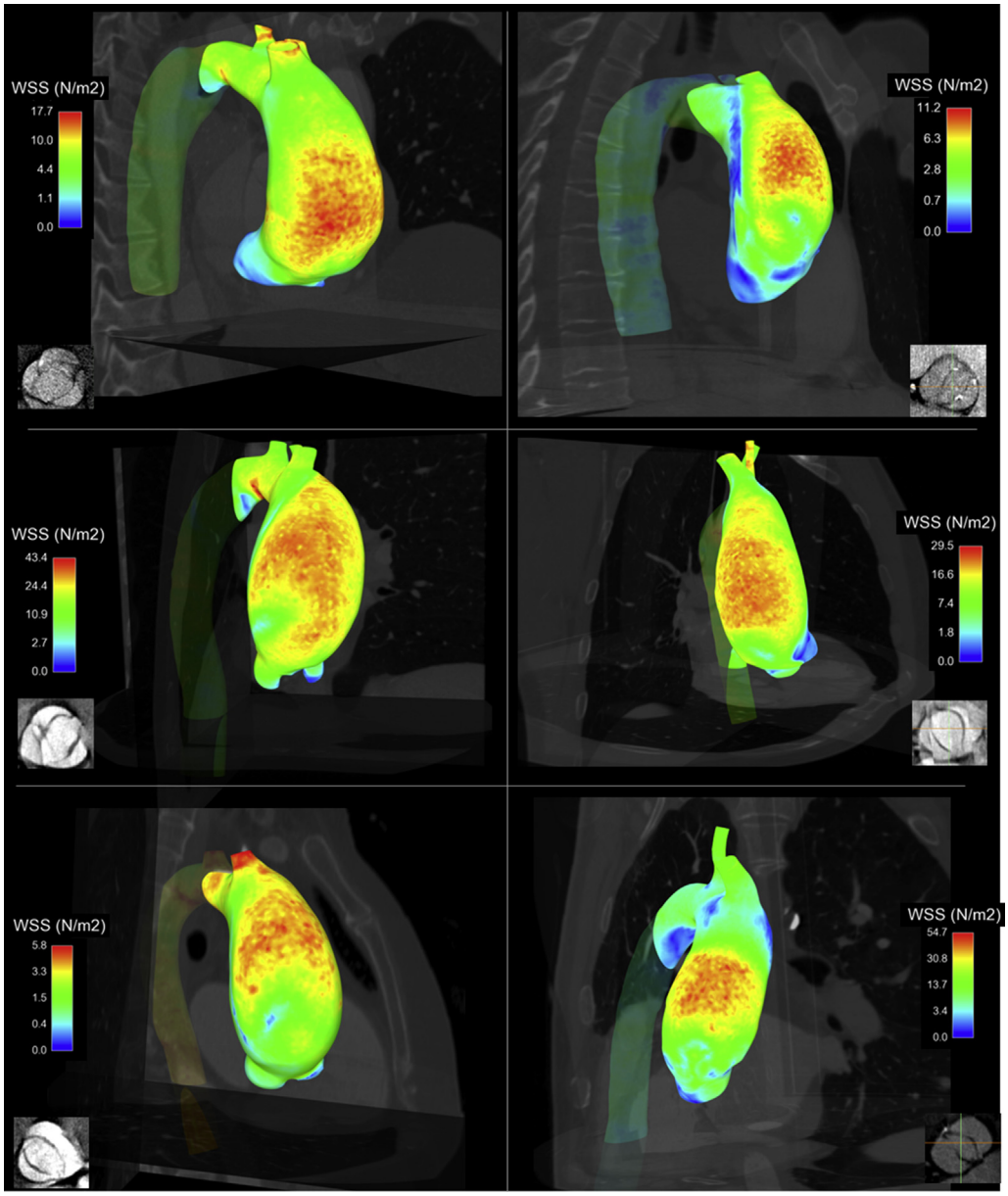

Figure 3. Systolic wall shear stress (WSS) distribution for patients with bicuspid aortic valve (BAV) type 1 and tubular aortic dilatation (row 1, left), BAV type 1 with diffusive aortic dilatation (row 1, right), BAV type 1 with tubular aortic dilatation (row 2, left), BAV type 2 with tubular aortic dilatation (row 2, right), BAV type 1 with tubular aortic dilatation (row 3, left), BAV type 2 with tubular aortic dilatation (row 2, left).

morphology of the aortic cusp fusion may increase local aortic wall shear stress causing adverse vascular remodelling and ultimately resulting in proximal dilatation of the ascending aorta. Indeed, it has recently been demonstrated that BAV patients are characterised by an extracellular matrix remodelling process that results in the degeneration of the elastic and collagen fibres within the aortic wall.[24] In these studies, histological observations indicated the likelihood of aortic wall damage near the region of increased WSSs, although this investigation was limited to few surgically repaired aortas seen during the period of investigation. A recent well designed study in a large patient cohort concluded that regions of increased WSSs as derived by 4D flow MRI are associated with extracellular matrix dysfunction and elastic fibre degeneration in the ascending aorta of BAV patients, supporting valve related haemodynamics as a mediator of bicuspid aortopathy.[25]

Four dimensional flow MRI allows the calculation of the first order derivative flow parameter (i.e., the WSS), from the spatial and temporal measurements of the three directional velocity field. Using this imaging technique, Mahadevia *et al.* showed that BAV type 1 results in increased WSSs in the right angular segment of the aortic wall (potentially leading to isolated tubular ascending aortic dilatation),[8] whereas BAV type 2 leads to increased WSS magnitudes in the posterior angular segment of the aortic wall (potentially leading to distal ascending aortic dilatation). The results of asymmetric WSSs in BAV type 1

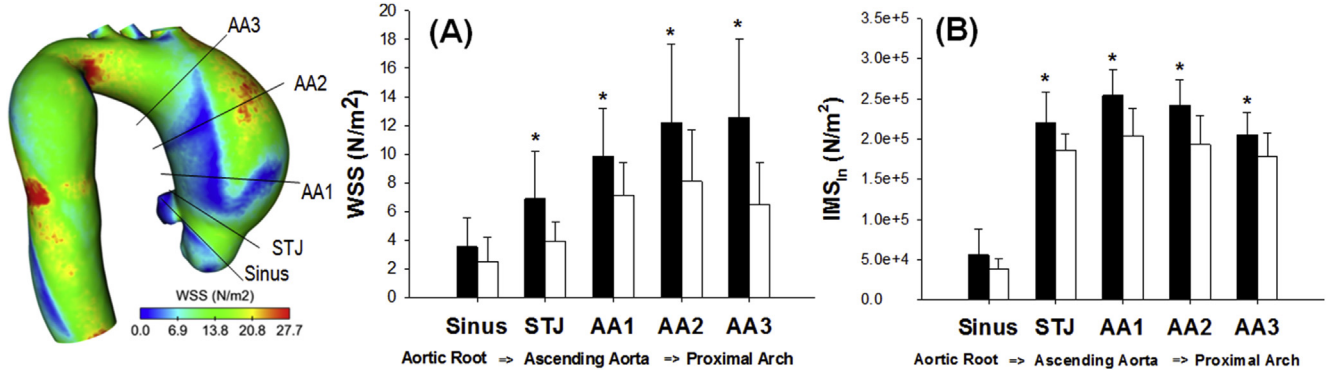

Figure 4. (A) Wall shear stresses (WSSs) and (B) inner aortic layer intramural stress (IMS_{IN}) for bicuspid aortic valve (BAV) patients (black bars) and tricuspid aortic valve (TAV) patients (white bars) at different analysis planes along the ascending aorta. *Note.* STJ = sinotubular junction. *Significantly different from TAV patient ($p < .05$).

versus BAV type 2 corresponded well to those estimated by 4D flow MRI. However, it should be noted that the accuracy of 4D flow MRI predictions is limited by a low spatial and temporal resolution of the velocity gradient at vessel edge. This probably explains the higher WSS magnitude found in the present study than those estimated by MRI. In practice, although 4D flow MRI can provide an *in vivo* estimation of the relative distribution of WSS, errors in gradient calculation can be large, and absolute magnitude of shear forces is not reliable.[26] Differently, WSS predictions from computational modeling are clearly advantageous as calculations of haemodynamics are performed at higher spatial resolution near vessel edge than that conceivable with 4D flow MRI. It is, however, recognised that computational modeling is complex and relies on theoretical assumptions on biomechanical properties and initial flow conditions, which are not common to 4D flow MRI. Therefore, computational modeling and 4D flow MRI have unique complimentary advantages and limitations so that the combination of these techniques should be advocated.

Study limitation

A few simplifications were made in the computational modelling approach. Material parameters and tissue thickness were assumed to be uniform along the ascending thoracic aorta, although the ascending aorta and aortic root have different mechanical properties and thicknesses. Moreover, material properties of aneurysmal aorta were not patient specific but rather population average values obtained from biomechanical testing of aortic tissue samples from patients with either BAV or TAV who underwent elective repair.[15] Resolution of the multiphoton technique is limited across the thickness so that fibre changes from the intimal to the adventitial aortic tissue surface may not have been fully captured. Material properties and fibre architecture changes along the longitudinal aortic direction were not modelled. The longitudinal stretch of the aorta induced by the heart motion and the zero pressure geometry of the vessel were not considered as these aspects may be challenging to model in fluid–structure interaction analyses. A clinical limitation was the inclusion of mild degrees of aortic regurgitation or stenosis (but not the combination of both

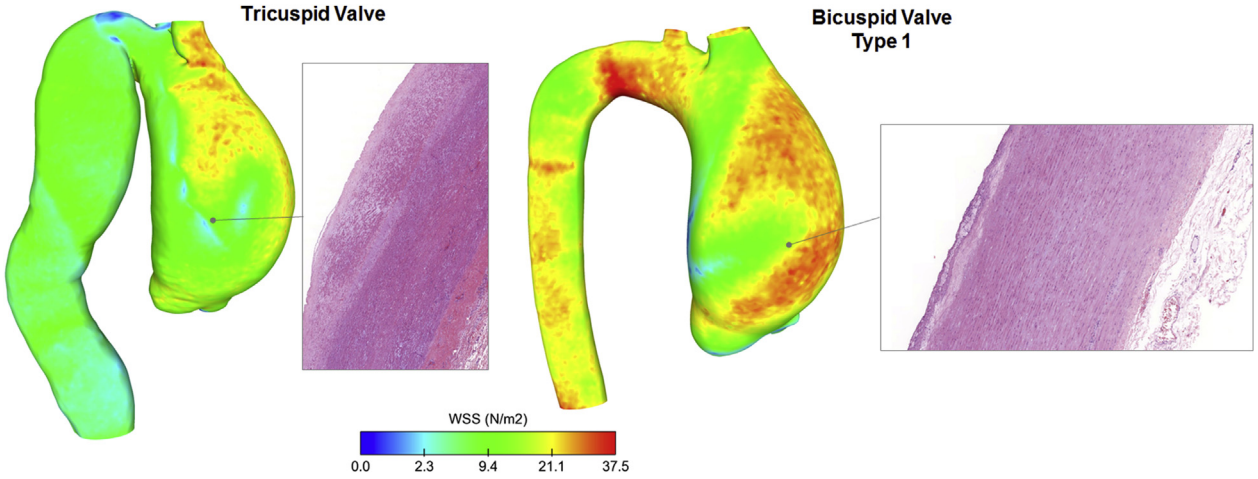

Figure 5. Haematoxylin and eosin histological observations (magnification 5×) of surgically resected tissue samples collected from region of increased systolic wall shear stress (WSS) for a tricuspid aortic valve patient (left) and a bicuspid aortic valve patient with type 1 phenotype and tubular aortic dilatation.

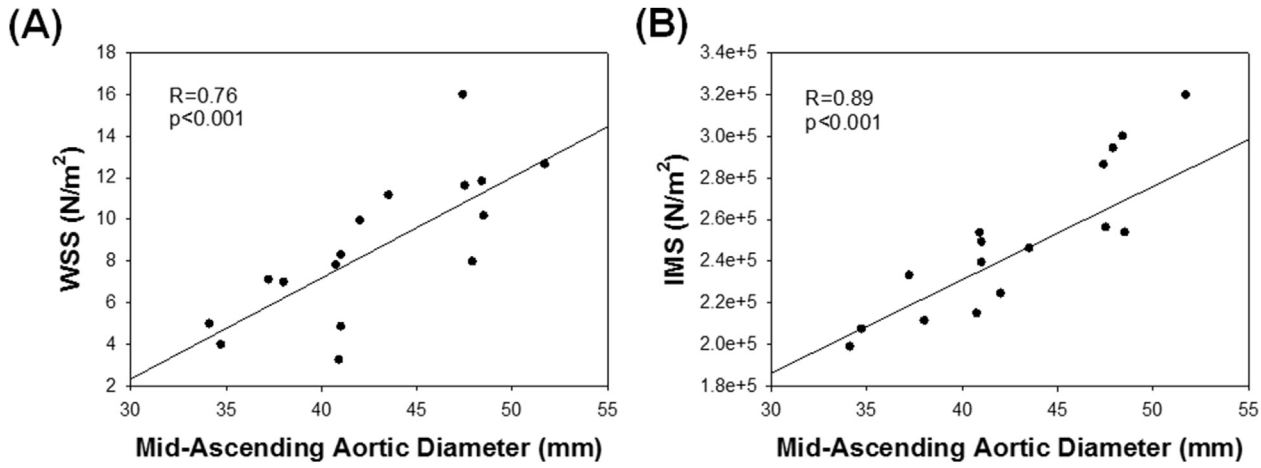

Figure 6. Plot showing positive correlation (A) between wall shear stress (WSS) and mid-ascending aortic diameter, and (B) between intramural stress (IMS) and mid-ascending aortic diameter; specifically the IMS of elective repaired aorta was within the indication for surgery.

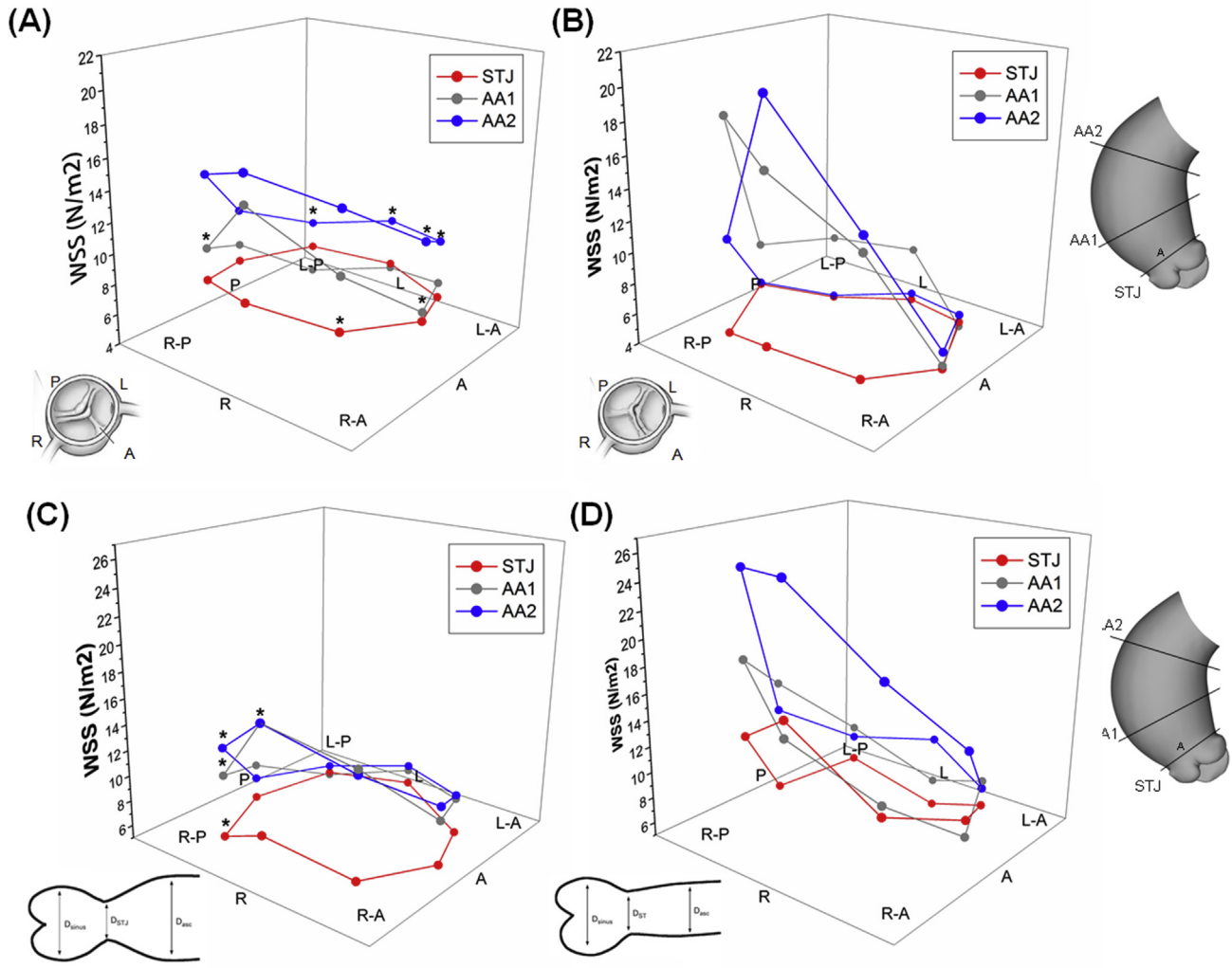

Figure 7. Mean values of segmental systolic wall shear stress (WSS) distribution at different planes of analysis for (A) bicuspid aortic valve (BAV) type 1 (A) versus (B) BAV type 2, as well as for (C) type A aortic shape versus (D) type E/N aortic shape across anatomical locations. *Note*. L = left; R = right; A = anterior; P = posterior; L-A = left-anterior; R-A = right anterior; L-P = left-posterior; R-P = right-posterior; STJ = sinotubular junction. *Significantly different from BAV type 2 ($p < .05$).

these valve related cofounding variables). Additionally, histological investigations of aortic tissue samples were limited to few representative cases. Inter-observer variability of aortic measurements and histological data were not investigated in this study.

CONCLUSIONS

The present study shows that BAV patients with preserved valvular functionality have significantly altered computationally derived wall shear and intramural stresses on the ascending thoracic aorta compared with TAV patients with comparable age and aortic size. Moreover, these computational parameters correlated with the aortic size. In addition, WSS was associated with asymmetric distribution along the aortic circumference with variable degree between different BAV phenotypes and aortopathy. Therefore, this study supports the use of non-size parameters to identify patient tailored indications and refine surveillance imaging criteria in BAV. However, future longitudinal studies are warranted to assess the correlation between the proposed haemodynamic and structural indices and aortopathy events, as well as the effect of these indices on proteomic changes, gene expression, and inflammatory changes in the aortic wall.

CONFLICTS OF INTEREST

None.

FUNDING

This work was supported by a “Ricerca Finalizzata” grant from the Italian Ministry of Health (GR-2011-02348129) to Salvatore Pasta.

REFERENCES

1 Fedak PW, Verma S, David TE, Leask RL, Weisel RD, Butany J. Clinical and pathophysiological implications of a bicuspid aortic valve. *Circulation* 2002;**106**(8):900—4.
2 Verma S, Siu SC. Aortic dilatation in patients with bicuspid aortic valve. *N Engl J Med* 2014;**370**(20):1920—9.
3 Tadros TM, Klein MD, Shapira OM. Ascending aortic dilatation associated with bicuspid aortic valve: pathophysiology, molecular biology, and clinical implications. *Circulation* 2009;**119**(6):880—90.
4 Uretsky S, Gillam LD. Nature versus nurture in bicuspid aortic valve aortopathy: more evidence that altered hemodynamics may play a role. *Circulation* 2014;**129**(6):622—4.
5 Sundt TM. Aortic replacement in the setting of bicuspid aortic valve: how big? How much? *J Thorac Cardiovasc Surg* 2015;**149**(2 Suppl.):S6—9.
6 Della Corte A, Bancone C, Dialetto G, Covino FE, Manduca S, Montibello MV, et al. The ascending aorta with bicuspid aortic valve: a phenotypic classification with potential prognostic significance. *Eur J Cardiothorac Surg* 2014;**46**(2):240—7.
7 Schaefer BM, Lewin MB, Stout KK, Gill E, Prueitt A, Byers PH, et al. The bicuspid aortic valve: an integrated phenotypic classification of leaflet morphology and aortic root shape. *Heart* 2008;**94**(12):1634—8.
8 Mahadevia R, Barker AJ, Schnell S, Entezari P, Kansal P, Fedak PW, et al. Bicuspid aortic cusp fusion morphology alters aortic three-dimensional outflow patterns, wall shear stress, and expression of aortopathy. *Circulation* 2014;**129**(6):673—82.
9 Kang JW, Song HG, Yang DH, Baek S, Kim DH, Song JM, et al. Association between bicuspid aortic valve phenotype and patterns of valvular dysfunction and bicuspid aortopathy comprehensive evaluation using MDCT and echocardiography. *JACC Cardiovasc Imag* 2013;**6**(2):150—61.
10 Pasta S, Rinaudo A, Luca A, Pilato M, Scardulla C, Gleason TG, et al. Difference in hemodynamic and wall stress of ascending thoracic aortic aneurysms with bicuspid and tricuspid aortic valve. *J Biomech* 2013;**46**(10):1729—38.
11 Rinaudo A, Pasta S. Regional variation of wall shear stress in ascending thoracic aortic aneurysms. *Proc Inst Mech Eng H* 2014;**228**(6):627—38.
12 Nathan DP, Xu C, Gorman III JH, Fairman RM, Bavaria JE, Gorman RC, et al. Pathogenesis of acute aortic dissection: a finite element stress analysis. *Ann Thorac Surg* 2011;**91**(2):458—63.
13 Nathan DP, Xu C, Plappert T, Desjardins B, Gorman 3rd JH, Bavaria JE, et al. Increased ascending aortic wall stress in patients with bicuspid aortic valves. *Ann Thorac Surg* 2011;**92**(4):1384—9.
14 Martin C, Sun W, Elefteriades J. Patient-specific finite element analysis of ascending aorta aneurysms. *Am J Physiol Heart Circ Physiol* 2015;**308**(10):H1306—16.
15 Pasta S, Phillippi JA, Gleason TG, Vorp DA. Effect of aneurysm on the mechanical dissection properties of the human ascending thoracic aorta. *J Thorac Cardiovasc Surg* 2012;**143**(2):460—7.
16 Pasta S, Phillippi JA, Tsamis A, D’Amore A, Raffa GM, Pilato M, et al. Constitutive modeling of ascending thoracic aortic aneurysms using microstructural parameters. *Med Eng Phys* 2016;**38**(2):121—30.
17 Kim HJ, Vignon-Clementel IE, Figueroa CA, LaDisa JF, Jansen KE, Feinstein JA, et al. On coupling a lumped parameter heart model and a three-dimensional finite element aorta model. *Ann Biomed Eng* 2009;**37**(11):2153—69.
18 Zamir M, Sinclair P, Wonnacott TH. Relation between diameter and flow in major branches of the arch of the aorta. *J Biomech* 1992;**25**(11):1303—10.
19 Morbiducci U, Ponzini R, Rizzo G, Cadioli M, Esposito A, De Cobelli F, et al. In vivo quantification of helical blood flow in human aorta by time-resolved three-dimensional cine phase contrast magnetic resonance imaging. *Ann Biomed Eng* 2009;**37**(3):516—31.
20 Shang EK, Nathan DP, Sprinkle SR, Fairman RM, Bavaria JE, Gorman RC, et al. Impact of wall thickness and saccular geometry on the computational wall stress of descending thoracic aortic aneurysms. *Circulation* 2013;**128**(11 Suppl. 1):S157—62.
21 Della Corte A, Bancone C, Conti CA, Votta E, Redaelli A, Del Viscovo L, et al. Restricted cusp motion in right-left type of bicuspid aortic valves: a new risk marker for aortopathy. *J Thorac Cardiovasc Surg* 2012;**144**(2):360—9.
22 den Reijer PM, Sallee 3rd D, van der Velden P, Zaaijer ER, Parks WJ, Ramamurthy S, et al. Hemodynamic predictors of aortic dilatation in bicuspid aortic valve by velocity-encoded cardiovascular magnetic resonance. *J Cardiovasc Magn Reson* 2010;**12**:4.
23 Hope MD, Hope TA, Meadows AK, Ordovas KG, Urbania TH, Alley MT, et al. Bicuspid aortic valve: four-dimensional MR evaluation of ascending aortic systolic flow patterns. *Radiology* 2010;**255**(1):53—61.
24 Tsamis A, Phillippi JA, Koch RG, Chan PG, Krawiec JT, D’Amore A, et al. Extracellular matrix fiber microarchitecture is

region-specific in bicuspid aortic valve-associated ascending aortopathy. *J Thorac Cardiovasc Surg* 2016;**151**:1718—1728.e5.
25 Guzzardi DG, Barker AJ, van Ooij P, Malaisrie SC, Puthumana JJ, Belke DD, et al. Valve-related hemodynamics mediate human bicuspid aortopathy: insights from wall shear stress mapping. *J Am Coll Cardiol* 2015;**66**(8):892—900.
26 Boussel L, Rayz V, Martin A, Acevedo-Bolton G, Lawton MT, Higashida R, et al. Phase-contrast magnetic resonance imaging measurements in intracranial aneurysms in vivo of flow patterns, velocity fields, and wall shear stress: comparison with computational fluid dynamics. *Magn Reson Med* 2009;**61**(2):409—17.

Eur J Vasc Endovasc Surg (2017) 54, 263

COUP D'OEIL

Ventriculo-caval Shunt Migration

M. Elens *, **P. Astarci**
Department of Cardiovascular and Thoracic Surgery, St Luc Hospital, Catholic University of Louvain, Brussels, Belgium

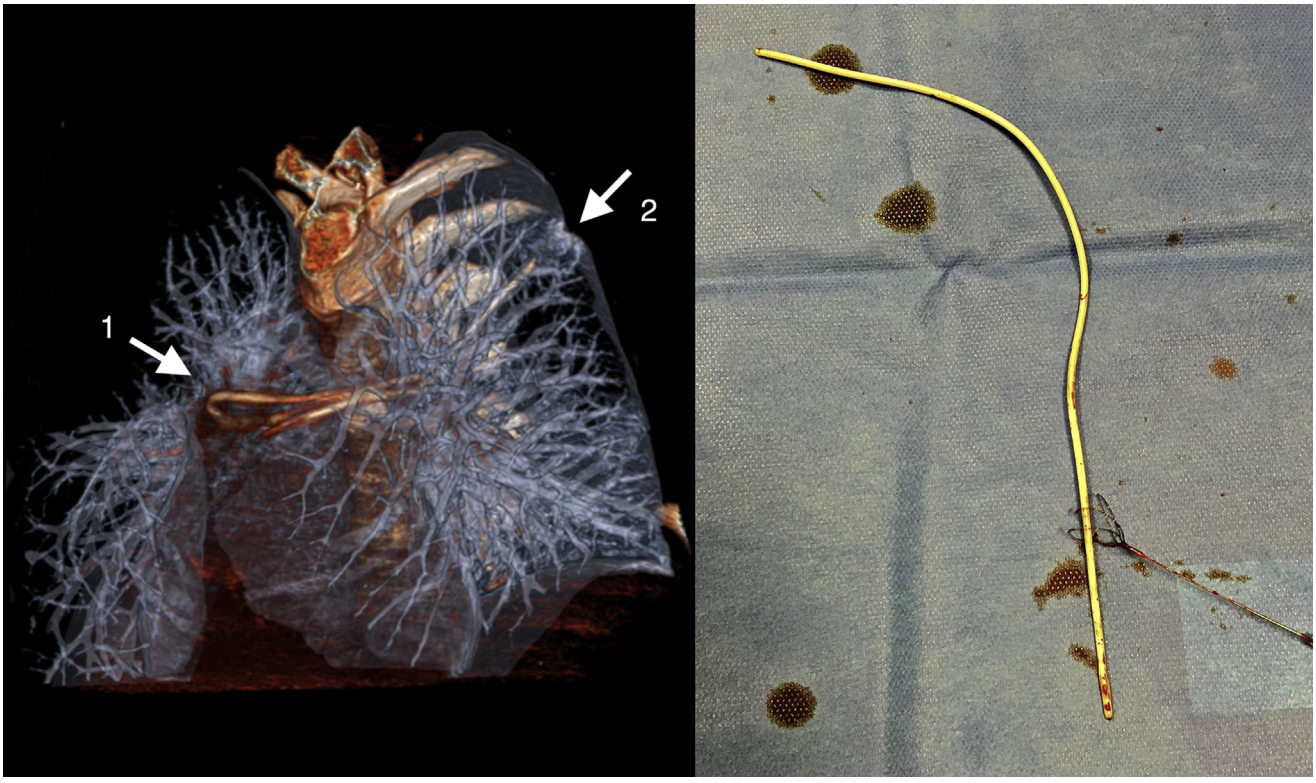

A 24 year old man with a previously inserted ventriculo-caval shunt (VCS) presented with diplopia and left hemithorax pain over 2 days. A brain CT scan showed a ventricular volume increase. During attempted VCS revision, migration of the shunt became apparent. A post-operative thoracic CT showed migration of the VCS into the pulmonary trunk and arteries (arrow 1) with an extension in a left segmental artery, causing a small intra-alveolar bleed (arrow 2). The shunt was successfully retrieved with an endovascular snare via femoral vein access. Diplopia and left hemithoracic pain were fully resolved 2 days after the procedure.

* Corresponding author. Avenue Hippocrate 10, 1200, Brussels, Belgium.
E-mail address: maxime.elens@uclouvain.be (M. Elens).

http://dx.doi.org/10.1016/j.ejvs.2017.04.007